The Overall Efficiency of Mixing in Exchange Flows through Lateral Contractions

Tjipto Prastowo*
Jurusan Fisika, FMIPA, Universitas Negeri Surabaya
Jl. Ketintang, Surabaya 60321

Abstract

Laboratory experiments are used to determine the overall (bulk) mixing efficiency in controlled exchange flows past a constriction. The flow generated in the laboratory channel is relevant to natural density-driven exchange flows commonly found in the oceans, where ocean straits control the exchange of waters of different density between adjacent ocean basins, between marginal seas and the open oceans, and within estuaries. The development of Kelvin-Helmholtz billows at the strongly sheared interface generates vertical mixing between the two opposing layers within the constriction. The amount of turbulent mixing is measured and converted to a mixing efficiency, defined as the fraction of the available energy released to kinetic energy of the flow that is converted into an irreversible increase in potential energy of the density field. For simple lateral contractions used in the experiments, the overall mixing efficiency is found to be constant at 11% for large Reynolds numbers, independent of all the external parameters and flow conditions. We conclude from the results that the average efficiency in the oceans is only half of that commonly used in ocean modeling.

KEYWORDS: mixing, exchange flows, lateral constarction

I. INTRODUCTION

Vertical mixing plays a key role in maintaining the abyssal ocean density stratification in the context of the global overturning ocean circulation [1]. The amount of available energy input required to sustain vertical mixing and the fraction of the input used for the mixing are poorly unknown [2]. Thus, it is important to quantify the rates at which turbulent mixing occurs in stably stratified turbulence. This study has therefore examined a specific class of flows of fundamental interest, namely buoyancy-driven, hydraulically-controlled exchange flows, in which accurate and precise measurements of the amount of irreversible mixing are possible to do in the laboratory. The change in the density structure of the water in the reservoirs is used to determine the mixing efficiency. The observed shear instability provides insights into the dynamics of mixing relevant to other forms of unstable shear flows. Similar exchange flows are also found in the oceans, where straits control the exchange of waters of differing densities between adjacent abyssal ocean basins [3, 4], between marginal seas and the open oceans [5, 6], and within estuaries [7].

In this study, mixing efficiency is defined as the fraction of the kinetic energy supplied to turbulence, which is in turn irreversibly converted into potential energy of the density field, while the remainder is viscously dissipated. Numerical simulations of the growth and collapse of a single Kelvin-Helmholtz (KH) billow [8, 9] have demonstrated a sequence of mixing events. In the simulations, a cumulative mixing efficiency is reported as the time-averaged efficiency, which has an asymptotic value of 0.15, less than the proposed value of 0.2 for stratified turbulence [10]. Other studies [11] have also investigated mixing efficiency in a linearly stratified fluid and found that the mixing efficiency of order 0.1 is possible.

Here, laboratory experiments are used to determine the overall efficiency of mixing in controlled exchange flows through topographic constrictions. The methods are detailed in section 2 and the background theory for mixing efficiency calculation is given in section 3. The experimental results for all cases are presented in section 4 and conclusions are given in section 5.

II. EXPERIMENTAL METHODS

A. Apparatus and Procedure

All experiments were conducted in a tank of length L = 5.26 m and width B = 0.2 m. Figure 1 shows the apparatus used in which one of four symmetric constrictions was placed at the centre of the channel. Three of the constrictions had curved walls, referred to as short constrictions (see Figure 1a, c), and the fourth with the same curved walls but included a straight central section, referred to as the long constriction (see Figure 1b, d), having parallel-sided walls 0.06 m apart and 0.5 m long (the total constriction length L_c was 1.0m). The minimum width bo of the short constrictions was such that the contraction aspect ratio b_o/B was 0.1, 0.3, or 0.5.

In each experiment, the tank was filled with freshwater to a depth of H and a removable barrier was inserted at the central point of the constriction. A density difference across the barrier was created by dissolving a measured quantity of salt into the right reservoir. Both the dense and light fluids were

*E-MAIL: t_prastowo@yahoo.com

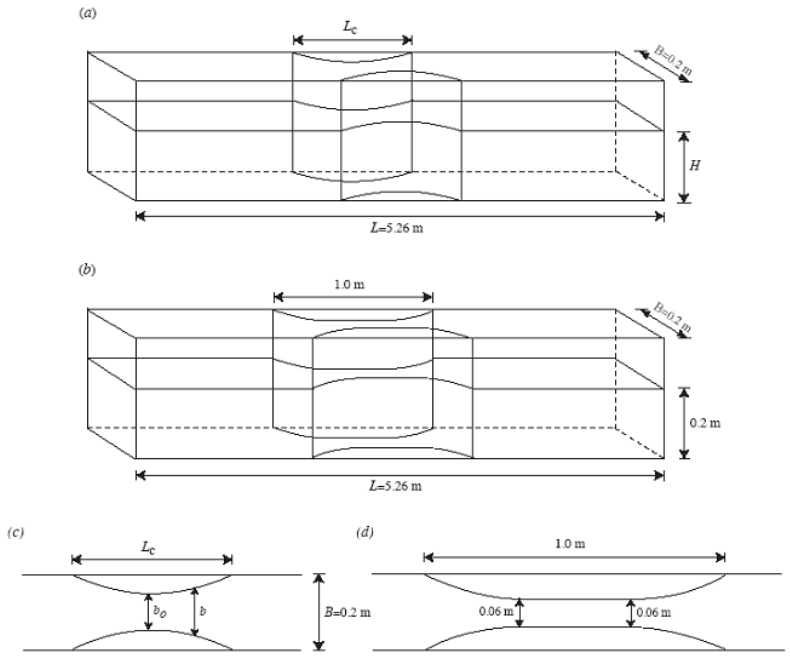

FIG. 1: Side view of a laboratory tank with (c) a short constriction; (d) a long constriction; and plan view of (a) a short constriction; (b) a long constriction.

dyed with different colours for flow visualisation. The reservoirs were then stirred thoroughly to ensure homogeneity in density. The free surface heights of both reservoirs were adjusted to give equal hydrostatic pressures at mid-depth so as to achieve a purely baroclinic exchange.

The exchange flow was initiated by the rapid removal of the barrier from the constriction over a period of approximately 1 second in each experiment. The barrier was then rapidly reinserted into the constriction at a time when gravity currents had nearly reached the far endwalls

B. Measurement Techniques

The initial densities of the fresh and saltwater reservoirs were measured in an Anton Paar digital density meter. The initial free surface heights in the reservoirs were determined to within $\pm$0.01mm using a digital micrometer gauge. After the exchange flow was stopped, the water was left to stand for at least two hours, long enough for all long waves to die away but too short for diffusion of salt to affect the density distribution in the reservoirs on length scales greater than 3mm. During this time, the tank was sealed to minimise evaporation. After each experiment, densities from both reservoirs were measured using the digital density meter to a precision of 10^{-3} kgm^{-3}. The final heights were also measured as required in the calculations of the final potential energies.

C. External Parameters

The relevant dynamic parameters include a fractional density difference $\Delta\rho_2/\rho_2 = (\rho_1 - \rho_2)/\rho_2$ (across the range 0.001 $\leq \Delta\rho_2/\rho_2 \leq$ 0.096), where ρ_1 and ρ_2 are the initial densities of the fresh and saltwater reservoirs, the reduced gravity g' = g $\leq \Delta\rho_2/\rho_2$, where g is acceleration due to gravity, the total water depth H and the kinematic viscosity ν. Flow conditions were examined by varying the flow aspect ratio H/L_c, the contraction aspect ratio b_o/B and a horizontal Reynolds number. The appropriate Reynolds number is based on the constriction length L_c, as this is the lengthscale for flow acceleration [12]. This number is referred to as the horizontal Reynolds number, defined as

$$R_e = \frac{0.5(g'H)^{1/2}L_c}{\nu} \quad (1)$$

lying in the range 1.2x104 $\leq$ Re $\leq$ 2.1x105 for all runs.

We carried out thirty runs with three different short constrictions and nine runs with a long constriction. For the short constrictions, the water depth H was set to 0.1 m, 0.2 m, or 0.3 m. The results for the short constrictions were compared with those for the long constriction, in which the water depth was fixed at 0.2m. These were aimed to examine the sensitivity of the results to the constriction geometry and water depth.

III. THEORY

Following [12], we describe a method of calculating the efficiency of mixing in a buoyancy-driven exchange flow. For

the initial state with two basins of homogeneous water of different density, the potential energy P_i is given by

$$P_i = g \int A\rho_1^{'} z dz_0^{h_1} + g \int A\rho_2^{'} z dz_0^{h_2} \qquad (2)$$

where h_1 and h_2 are the initial free surface heights of the fresh and saltwater reservoirs, respectively, and A is the horizontal cross-section of each reservoir, which may be either uniform or dependent on height.

In the final state after the exchange and mixing have occurred and altered the properties of water on both sides of the constriction, the potential energy P_f is determined by the measured density distribution, ρ_1' and ρ_2, in both reservoirs,

$$P_f = g \int A\rho_1^{'}(z) dz_0^{h_1'} + g \int A\rho_2^{'}(z) dz_0^{h_2'} \qquad (3)$$

where h_1 and h_2 are the final free surface heights of the fresh and saltwater, reservoirs, respectively, and again A is the cross-sectional area in each reservoir.

We examine the effects of mixing by defining the hypothetical minimum state that would be present if mixing did not occur. This hypothetical state is obtained by redistributing the measured total amount of salt within each reservoir into fresh and saltwater layers of densities ρ_1' and ρ_2. We write the required thicknesses of the fresh and saltwater layers in each of the reservoirs for this state as h_{fi} (i = 1, 2) and h_{si} (i = 1, 2), respectively. We assume a linear equation of state such that $h_i = h_{si} + h_{fi}$, giving constant volume. The hypothetical minimum potential energy P_h is then given by

$$\begin{aligned} P_h = \quad & g \int A\rho_2 z dz_0^{h_{s1}'} + g \int A\rho_1 z dz_{h_{s1}}^{h_1'} \\ + \ & g \int A\rho_2 z dz_0^{h_{s2}'} + g \int A\rho_1 z dz_{h_{s2}}^{h_2'} \end{aligned} \qquad (4)$$

The potential energy increase owing to mixing, or the amount of mixing, P_m is the difference in potential energies between the final state and hypothetical state with no mixing, $P_m = P_f - P_h$. The available potential energy P_a released to the flow is the difference in potential energies between the initial and hypothetical states, $P_a = P_i - P_h$. We define the mixing efficiency as the fraction of the available potential energy released to kinetic energy of the flow that is transformed into an irreversible increase in the potential energy of the density distribution above the hypothetical state. The mixing efficiency η for a two-layer exchange flow can then be written as

$$\eta = \frac{P_m}{P_a} = \frac{P_f - P_h}{P_i - P_h} \qquad (5)$$

where the denominator P_a is the total mechanical energy supplied. Thus, η in (5) represents the overall efficiency with which mixing draws on the available energy in this type of flow.

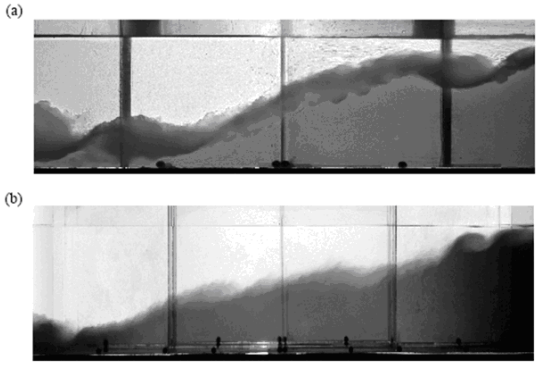

FIG. 2: Intense mixing in the vicinity of the constriction from two different experiments. Panel (a) shows an experiment with a short constriction having b_o =100 mm, H = 0.2 m, $\Delta\rho/\rho_2$ = 6.7% and R_e = 7.2x10^4, while panel (b) shows an experiment using a long constriction having b_o = 60 mm, H = 0.2 m, $\Delta\rho/\rho_2$ = 4.8% and R_e = 15.5 x 10^4. The mean flow within the constriction in both cases is steady.

IV. EXPERIMENTAL RESULTS

A. Qualitative Observations

After the barrier was removed, the subsequent density-driven exchange flow led to shear instability and extensive mixing, particularly in the vicinity of the constriction (see Figure 2). Hydraulic jumps occurred near the exits of the constriction and gravity currents formed in each reservoir to accommodate the exchange. The flow was characterised by the growth and collapse of KH billows on the strongly sheared interface within the contraction, generating overturns and vertical mixing. These billows, along with the resulting mixed fluid, were carried away from the centre of the constriction and were not present beyond the hydraulic jumps.

There were no persistent billows along the stratified region above the gravity currents, apart from those on the current heads. The exchange was stopped as the barrier was replaced into the channel at a time when the current noses had nearly reached the endwalls. Thus, throughout the exchange the mean flow in the constriction was in a steady state and the distant endwalls had no influence on the flow.

After the barrier was reinserted, the currents were reflected from the far endwalls to form large-amplitude waves, which propagated towards the constriction and were reflected back from the replaced barrier, after which a complex pattern of wave-wave interactions was observed in each reservoir. All of these processes produced a relatively minor amount of mixing.

There were no qualitative differences in the flow for experiments with large Reynolds numbers. Continuous overturning at the sheared interface within the constriction was the dominant feature in these experiments. In experiments with low Reynolds numbers, the shear instability at the interface appeared to be relatively weak and the billows were only intermittent, with consequently weak mixing between the layers.

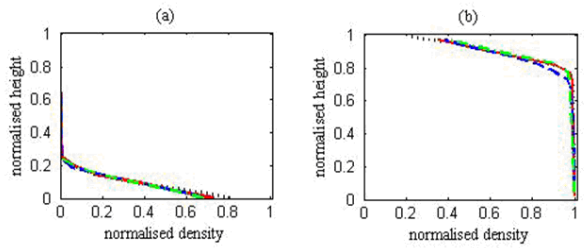

FIG. 3: The normalised profiles $(\rho_z - \rho_1)/)\rho_2 - \rho_1)$, plotted against normalised height z/H in experiments with a short constriction. Frames (a) and (b) are the left and right profiles measured from experiments with H = 0.2 m, b_o = 20 mm and four different fractional density differences: $\Delta\rho/\rho_2$ = 0.7% (dotted line), $\Delta\rho/\rho_2$ = 1.9% (solid line), $\Delta\rho/\rho_2$ = 3.0% (dashed line) and $\Delta\rho/\rho_2$ = 4.8% (dashed-dotted line), respectively.

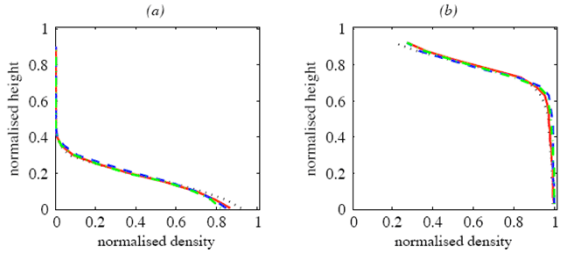

FIG. 4: The normalised profiles $(\rho_z - \rho_1)/)\rho_2 - \rho_1)$, plotted against normalised height z/H in experiments with a long constriction. Frames (a) and (b) are the left and right profiles measured from experiments with H = 0.2 m, b_o = 60 mm and four different fractional density differences: $\Delta\rho/\rho_2$ = 0.7% (dotted line), $\Delta\rho/\rho_2$ = 1.9% (solid line), $\Delta\rho/\rho_2$ = 3.0% (dashed line) and $\Delta\rho/\rho_2$ = 4.8% (dashed-dotted line), respectively.

B. The Density Profiles

Here we provide normalised final density profiles measured from both the left and right reservoirs after each experiment from cases with short and long constrictions. In each case, the depth is normalised by the full water depth H and the density is normalised by the initial difference in the densities of both reservoirs. The normalised density sets to zero at the water surface and to unity at the channel base.

Examples of the normalised profiles from both reservoirs measured at the end of an experiment using a short constriction are plotted in Figure 3. The profiles show four experiments having the same water depth (H=0.2m) and constriction minimum width (b_o = 20 mm), but with different fractional density differences $\Delta\rho/\rho_2$ (see detailed differences in the figure caption).

Examples of the density profiles from the long constriction case are plotted in Figure 4 for four experiments having the same constriction minimum width (b_o = 60 mm) and water depth (H = 0.2 m), but with different fractional density differences $\Delta\rho/\rho_2$ (see detailed differences in the figure caption). It is clear that the normalised profiles for the left (see Figure 3a and 4a) and right reservoirs (see Figure 3b and 4b) are similar to each other, suggesting that flow processes are dynamically similar in both cases. This implies that mixing efficiency is likely to be the same for both the short and long constricitons (see also Figure 5 for the results of the measured efficiencies). Likewise, Figure 3 and 4 suggest that mixing processes in each reservoir are the same for both cases. This is what we call as symmetric mixing in channels of constant depth, but varying width.

C. The Measured Efficiencies

We also provide an overview of all experiments conducted by plotting in Figure 5 the results for all cases. The resulting mixing efficiencies for both the short and long constriction cases approach an asymptotic value of η = 0.11 at large Re (shown as the solid line in Figure 5). In experiments with low

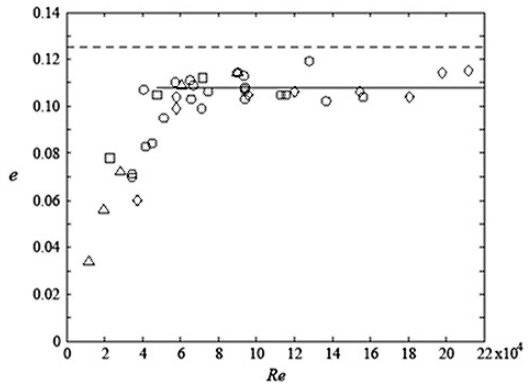

FIG. 5: The measured mixing efficiencies η as a function of the horizontal Reynolds number R_e for all cases. Symbols indicate b_o = 20 mm (circles), 60 mm (triangles) and 100 mm (squares) for the short constrictions, and b_o= 60 mm (diamonds) for the the long constriction. The dashed and solid lines show the theoretical value (η = 0.125) for the mixing efficiency and the mean (η = 0.108) of the measured efficiencies for $R_e > 5$ x 10^4, respectively.

Reynolds numbers, smaller efficiencies are, however, measured. Control experiments were carried out to examine the effects of the non-linear equation of state of salt solutions, particularly at large density differences, where mixing tends to decrease the total volume and increase the internal energy, thus reducing the increase in potential energy owing to mixing. However, the influence of these effects on the calculated efficiency was found to be 0.005, smaller than the uncertainty of the measurements. Hence, we have assumed in all calculations that the density depends linearly upon salinity and that non-linear mixing has a negligible effect on the measured efficiencies.

We also conducted experiments with various run times to include runs in which the barrier was replaced into the channel after the gravity current heads had reflected from the far endwalls. These runs, along with those with the barrier was reinserted before the current noses had reached the endwalls, were designed to examine time-dependent mixing (not detailed here). The results confirm that the rate of mixing was

constant for the steady exchange flow and that mixing associated with the starting and ending of the exchange flow by lifting and replacing the barrier had no significant contributions to the overall amount of mixing.

V. CONCLUSION

We have performed laboratory experiments to determine the overall (bulk) mixing efficiency in hydraulically-controlled, two-layer steady exchange flows through short and long constrictions. In the laboratory channel, we have found that the steady shear at the interface between the layers leads to the generation of KH billows and persistent, small-scale turbulence within the constriction. The most obvious effect of mixing in all cases is the production of the substantial volume of mixed water in the reservoirs after the experiment. The experimental methods developed provide a measure of the cumulative, irreversible mixing over time and length scales large compared with the turbulent events, which leads to the calculations of the bulk mixing efficiency.

The dependence of mixing efficiency on the details of constriction geometry and flow conditions has been examined in detail for a range of external parameters. For the short and long constrictions used in the experiments, the overall efficiency asymptotes to a constant value of 0.11 ($\pm$0.01) at large R_e, independent of all the external parameters. These results are consistent with the theoretical upper bound prediction for the mixing efficiency of 0.125 for the steady exchange flows. However, in experiments with low Reynolds numbers, we find that the shear instability is less efficient at mixing, owing to the absence of continuous small-scale turbulence at the interface, leading to smaller values of the measured efficiencies.

The results are expected to be applicable to the large-scale oceanic flows as these flows are associated with flows with large R_e. The mixing efficiency for such flows approaches the theoretical upper bound of the efficiency, which is 0.125, fairly close to 0.15 obtained from numerical simulations [8, 9]. The results provide insights into a broader range of density-stratified shear flows. While the results are supported by theoretical work [11], there remains discrepancies between the current results and those of previous studies [13, 14]. These studies have found that the asymptotic value of mixing efficiency is approximately 0.2, commonly referred to as the mixing efficiency for steady, turbulent shear flows [10], used in the general ocean circulation model [1, 2]. However, the smaller asymptotic value obtained here raises the possibility that the average mixing efficiency in the oceans may not be as large as widely assumed and that the calculations of the global energy balance of the oceans need reevaluated.

Acknowledgments

This study is part of the author's PhD project in the field of Earth Physics at Research School of Earth Sciences (RSES), The Australian National University (ANU). The author would like to thank Prof. Ross Griffiths, Dr. Graham Hughes and Dr. Andy Hogg for their best guidance and support. Tony Beasley and Brad Ferguson are helpful for their technical assistance during the completed work.

[1] W. Munk and C. Wunsch, *Abyssal recipes II: energetics of tidal and wind mixing*, Deep Sea Research I, **45**, pp. 1977-2010, 1998.
[2] C. Wunsch and R. Ferrari, *Vertical mixing, energy, and the general circulation of the oceans*, Annual Review of Fluid Mechanics, **36**, pp. 281-314, 2004.
[3] R. R. Dickson and J. Brown, Journal of Geophysical Research, **99**, pp. 12319-12341 (1994).
[4] H. L. Bryden and A. J. G. Nurser, Journal of Physical Oceanography, **33**, pp. 1870-1872 (2003).
[5] N. Bray, W. J. Ochoa, and T. Kinder, Journal of Geophysical Research, **100**, pp.10755-10776 (1995).
[6] M. C. Gregg and E. Ozsoy,Journal of Geophysical Research, **107**, 10.1029/2000JC000485 (2002).
[7] H. Stommel and H. Farmer, Journal of Marine Research, **12**, pp. 13-20 (1953).
[8] C. P. Caulfield and W. Peltier, Journal of Fluid Mechanics, **413**, pp. 1-47 (2000).
[9] W. Peltier and C. P. Caulfield, Annual Review of Fluid Mechanics, **35**, pp. 135-167 (2003).
[10] T. R. Osborn, Journal of Physical Oceanography, **10**, pp. 83-89 (1980).
[11] L. Arneborg, Journal of Physical Oceanography, **32**, pp. 1496-1506 (2002).
[12] T. Prastowo, R. Griffiths, G. Hughes, and A. Hogg, Journal of Fluid Mechanics, **600**, pp. 235-244 (2008).
[13] J. Imberger and G. N. Ivey, Journal of Physical Oceanography, **21**, pp. 659-680 (1991).
[14] P. Monti, G. Querzoli, A. Cenedase, and S. Piccinini, Physics of Fluids, **19**, 085104 (2007).